Searching for hidden matter
with long-range angular correlations at e^+e^- colliders

Redamy Pérez-Ramos[1,2,*], Miguel-Angel Sanchis-Lozano[3,†] and Edward K. Sarkisyan-Grinbaum[4,5,‡]

[1]*DRII-IPSA, Bis, 63 Boulevard de Brandebourg, 94200 Ivry-sur-Seine, France*
[2]*LPTHE, Sorbonne Université, UPMC Univ Paris 06, UMR 7589, F-75005, Paris, France*
[3]*Instituto de Física Corpuscular (IFIC) and Departamento de Física Teórica Centro Mixto Universitat de València-CSIC, Dr. Moliner 50, E-46100 Burjassot, Spain*
[4]*Experimental Physics Department, CERN, 1211 Geneva 23, Switzerland*
[5]*Department of Physics, The University of Texas at Arlington, Texas 76019, USA*

The analysis of azimuthal correlations in multiparticle production can be useful to uncover the existence of new physics beyond the Standard Model, e.g., Hidden Valley, in e^+e^- annihilation at high energies. In this paper, based on previous theoretical studies and using the PYTHIA8 event generator, it is found that both azimuthal and rapidity long-range correlations are enhanced due to the presence of a new stage of matter on top of the QCD partonic cascade. Ridge structures, similar to those observed in hadronic collisions at the LHC, show up providing a possible signature of new physics at future e^+e^- colliders.

I. INTRODUCTION

In a series of previous papers, particle correlations were used to extract information about intrajet multiparticle dynamics [1], and for the search of new physics beyond the Standard Model (SM) in hadronic high-energy collisions [2,3]. Indeed, the analysis of long-range particle correlations can provide useful information about the early stage of matter and shed light on the possible presence of new physics on top of the QCD parton shower. On the other hand, e^+e^- collisions should provide to this end a much cleaner environment than hadron colliders, as well as a definite (though adjustable) center-of-mass energy.

The analyses of two-particle angular correlations in high-multiplicity proton-proton, proton-nucleus, and heavy-ion collisions, have revealed a ridge structure of final state hadrons emitted almost collinearly within a broad rapidity difference [4–6]. Different theoretical explanations have been put forward to explain this initially unexpected phenomenon, almost of all them requiring the existence of some unconventional state of matter at the beginning of the collision, e.g., the quark-gluon plasma [7–9] and/or glasma [10,11].

Analogies can be found in the Cosmic Microwave Background [12] where the inflationary epoch plays the role of a hidden sector similarly stretching correlations at large angles.

This paper focuses on Hidden Valley (HV) models [13], with a new relatively light hidden sector weakly connecting to the SM. Actually, the HV scenario encompasses a variety of theoretical frameworks from stringlike [14] to unparticle models [15]. This paper mainly deals with QCD-like models where new types of particles, v-quarks, undergo new (strong) interactions mediated by HV photons (γ_v) or HV gluons (g_v) [16].

The simplest way of coupling the SM and the Hidden Sector (HS) occurs via a heavy Z_v of mass $\gtrsim 1$ TeV, i.e., $e^+e^- \to Z_v^* \to$ hadrons. Another possibility involves mirror partners of the SM quarks (Q_v) and leptons (E_v) collectively denoted as F_v, charged under both SM and HS, thereby with the capacity of connecting both sectors. Note, however, that this notation, stressing the parallelism between both SM and HV sectors, should not be pushed too far as F_v can be either a fermion or a boson.

Hence, both Q_v and E_v mediators can be pair produced via the annihilation process $e^+e^- \to \gamma^* Z^{0*} \to F_v \bar{F}_v$ above energy threshold, subsequently decaying back into SM particles. Note that this paper only concerns pair production of Q_v, but not E_v, as the hadron-production cross section is smaller for the latter than the former by about one order of magnitude. Moreover, hadron multiplicity should be significantly larger in $Q_v \bar{Q}_v$ production because of expected softer color fields in the $E_v \bar{E}_v$ case along the parton shower due to the replacement of quarks by leptons.

*redamy.perez-ramos@ipsa.fr
†Miguel.Angel.Sanchis@ific.uv.es
‡Edward.Sarkisyan-Grinbaum@cern.ch

The allowed Q_v content in a typical HV scenario are denoted here as D_v, U_v, S_v, C_v, B_v, and T_v, in correspondence with the SM flavors. In the present paper, the main focus is given to the lightest and heaviest cases, namely, to D_v of mass $\simeq 100$ GeV and T_v of several 100 GeV, while intermediate masses lead to intermediate results.

Three kinds of partonic showers, ultimately yielding final-state SM particles, are distinguished here:

(i) $e^+e^- \to q\bar{q} \to$ hadrons, where q collectively denotes all quark flavors below the top (t) mass. Using the PYTHIA8 event generator [17,18], all flavors are generated according to the respective production cross sections.

(ii) $e^+e^- \to t\bar{t} \to$ hadrons. Top quark possesses special interest because of its very large mass and the fact that it does not form bound states but promptly decays into lighter particles, mimicking to some extent the extra cascade due to an extra hidden sector.

(iii) $e^+e^- \to Q_v\bar{Q}_v \to$ hadrons [16], i.e., HV pair-production, the main goal of this study. Let us stress that decay modes like $g_v \to g_v\bar{g}_v$, $g_v \to q_v\bar{q}_v$, and $\gamma_v \to q_v\bar{q}_v$ are similar to SM processes along the partonic cascade before hadronization involving equivalent parameters (like the strong coupling constant) to be developed below.

II. MONTE CARLO STUDY

The current analysis rests on two bases: (a) a previous theoretical study of two-particle and three-particle correlations developed by two authors [3,19,20], where the possible HV contribution beyond the SM is incorporated on top of the parton shower, and (b) a Monte Carlo (MC) study using PYTHIA8 [17,18] with different HV sectors incorporated. The MC study here explores the HV scenario letting some parameters of particular relevance vary along wide intervals of model parameters. For example, the masses of the v-partners (m_{q_v}) of the SM fermions were set along the interval [10, 100] GeV. The corresponding (nonrunning) coupling constant α_v was set from the (default in PYTHIA) value $\alpha_v = 0.1$ up to $\alpha_v = 0.8$, while lower cutoff for shower evolution was taken the same as in QCD, i.e., 0.4 GeV. All other model parameters, such as the spin and widths of the HV mediators and v-quarks, were taken by default in PYTHIA as well. In all these cases, it has been checked explicitly that the MC output (e.g., two-particle correlation heights and lengths) changed within about 20%. Consequently, only some plots for representative choices of those parameters are shown here.

Table I displays some production cross sections, σ, for several representative channels in SM and HV scenarios, as obtained as a PYTHIA output. As can be seen, the HV cross sections are about 10–100 smaller than the SM ones, without taking into account detector effects or any kind of selection cuts applied on events. The values shown in

TABLE I. Inclusive cross sections in e^+e^- collisions for different production channels and center-of-mass energies.

Final states:	Light quarks	$t\bar{t}$	$D_v\bar{D}_v$	$T_v\bar{T}_v$
σ (pb) at 250 GeV	312	$\cdots$	4.5	$\cdots$
σ (pb) at 350 GeV	24.1	2.1	1.8	$\cdots$
σ (pb) at 800 GeV	69.5	44.4	1.4	1.2

Table I are encouraging. A more detailed consideration of the signal-to-background ratio is left for further investigations.

In what follows, particle correlations are studied as a function of rapidity and azimuthal angle in e^+e^- annihilations at different center-of-mass energies ($\sqrt{s} = 250$–800 GeV, as foreseen in future e^+e^- colliders) using the sphericity frame.

The choice of this reference frame is especially suitable in e^+e^- colliders [21,22] since the sphericity axis coincides with the averaged outgoing direction of the back-to-back $q\bar{q}$ jets produced in the annihilation process.

A. Two-particle azimuthal correlations

The two-particle correlation function represents the ratio of the number of charged particle pairs from the same event (signal), and that from different events (background),

$$C_2(\Delta y, \Delta\phi) = \frac{S_2(\Delta y, \Delta\phi)}{B_2(\Delta y, \Delta\phi)}, \qquad (1)$$

with the differences on rapidity and azimuthal angles of particles 1 and 2, $\Delta y \equiv \Delta y_{12} = y_1 - y_2$ and $\Delta\phi \equiv \Delta\phi_{12} = \phi_1 - \phi_2$ as used in experiments [4–6,23,24].

Based on general physical grounds (causality), a near-side ridge may be expected in such a 3-dimensional plot of the C_2 function, very much like the one appearing in hadronic collisions. This is because of the assumed formation of a nonconventional stage of matter just after the collision on top of the conventional QCD cascade, thereby extending the angular correlation length as theoretically anticipated for hadronic collisions in [19]. This important issue is addressed below by studying three-particle correlations, while here two-particle correlations are examined in different scenarios and parameter choices.

In Fig. 1, the $C_2(\Delta y, \Delta\phi)$ function is plotted as defined in Eq. (1). The most striking difference lies on the existence of long-range, near-side angular correlations (ridge [4]) within $2 < |\Delta y| < 4$ at $\Delta\phi \approx 0$ for the HV scenario. This structure was checked to hold to a different extent for other Q_v cases while only the D_v is plotted.

Figure 2 displays the transverse-plane cuts along collinear particle pairs ($\Delta\phi \approx 0$) of all panels of Fig. 1 to highlight the observed differences. A near-side ridge may unveil the existence of this type of event ($D_v \to d + q_v$) away and near the resonant mass of the D_v quark
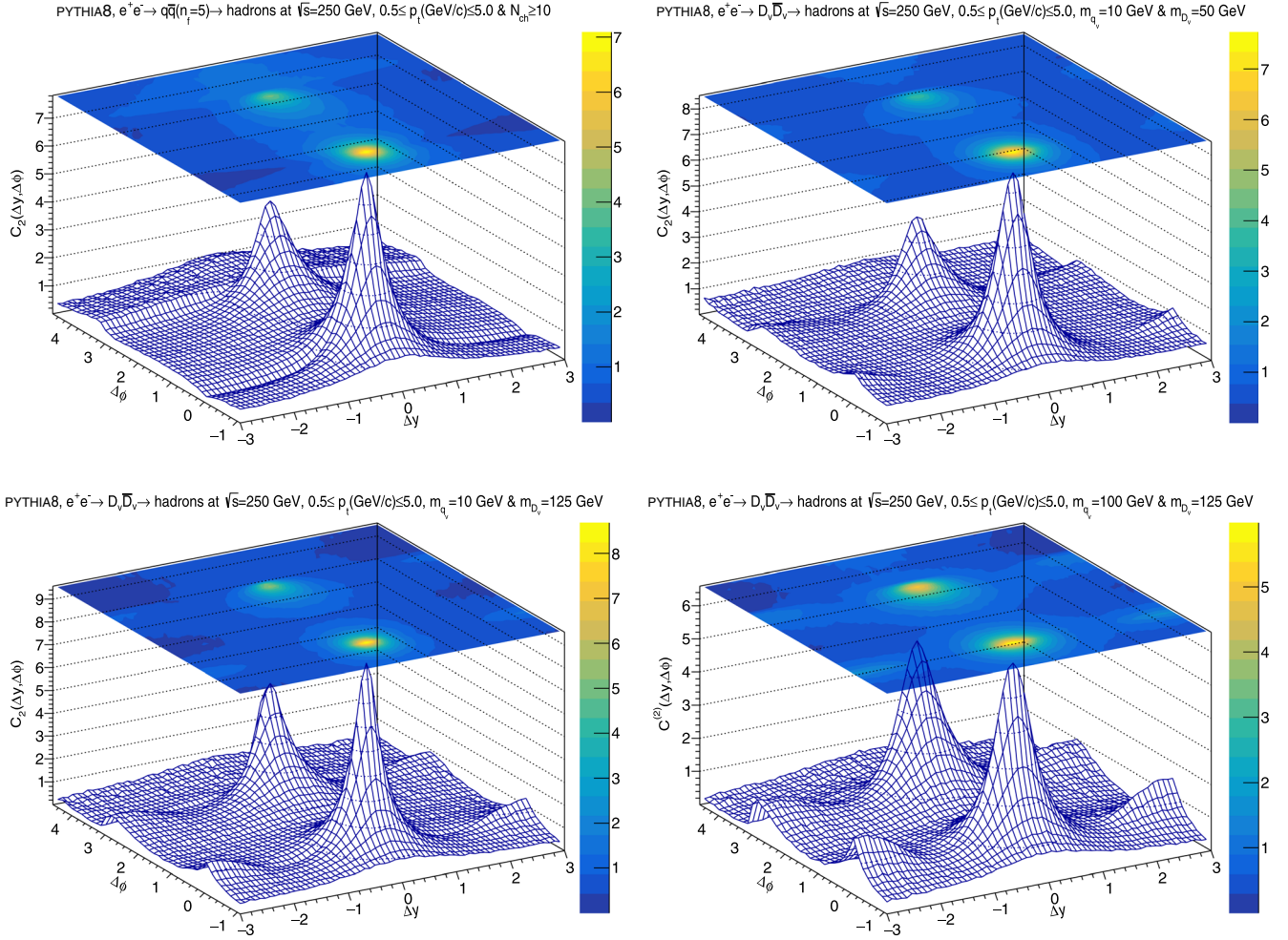
FIG. 1.   Two-particle correlation function $C_2(\Delta y, \Delta \phi)$ in azimuthal angle and rapidity for the $e^+ e^-$ annihilation, generated with PYTHIA8 at $\sqrt{s} = 250$ GeV. Top left panel: Standard Model (SM) process with all quark species except top; top right panel: Hidden Valley (HV) scenario with a v-quark of mass $m_{q_v} = 10$ GeV and the D_v mass of the HV mirror partner to SM d-quark, $m_{D_v} = 50$ GeV; bottom left panel: HV scenario with $m_{q_v} = 10$ GeV and $m_{D_v} = 125$ GeV; bottom right panel: HV scenario with $m_{q_v} = 100$ GeV and $m_{D_v} = 125$ GeV. Here, n_f is the number of SM flavors, q denotes all quark species except the top quark, N_{ch} is the number of charged particles, and p_t stands for the transverse momentum of the produced particles in the sphericity frame.

($m_{D_v} = 50$–125 GeV). In this region, quasicollinear ($\Delta \phi \approx 0$) particle pairs with delayed rapidities are the most copiously collected compared to SM processes. Indeed, as a consequence of the D_v decay products, a hadron triggered by the SM d quark (of a rather modest mass) yields a larger rapidity than a hadron triggered by the much heavier q_v partner of mass $m_{q_v} = 10$–100 GeV, in agreement with the 3-dimensional plots. In addition, the ridge turns out to be highest for the heaviest v-quark here considered, i.e., $m_{q_v} = 100$ GeV. Hence, it can be concluded that such a ridge is not produced by the SM cascade, so it becomes particularly suggestive to interpret the appearance of the ridge phenomenon in $e^+ e^-$ collisions as a consequence of a new stage of matter on top of the QCD parton cascade. In fact, this is one of the main assumptions of this study, which is examined below using three-particle correlations.

Furthermore, a narrow peak can be seen for $\Delta y \approx 0$ and $\Delta \phi \approx 0$ arising from particle pairs inside the same events, and the away-side ridge (at $\Delta \phi \approx \pi$) typically due to back-to-back jet production as a consequence of energy-momentum conservation. It is worth mentioning that the latter clearly exhibits stronger correlations in the HV sector than those in the SM, as visible from the plots. Note that the essential features of the equivalent plot, obtained by ALEPH [23] and Belle [24] experiments are reproduced while using the thrust axis.

Figure 3 shows the 3-dimensional plot of the two-particle correlation function $C_2(\Delta y, \Delta \phi)$ for SM top quark production in $e^+ e^- \to \gamma^*/Z^0 \to t\bar{t} \to$ into hadrons, and HV down-type quark production $e^+ e^- \to \gamma^*/Z^* \to D_v \bar{D}_v \to$ hadrons at $\sqrt{s} = 350$ GeV.

The away-side ridge in Fig. 3 (left panel) shows much lower back-to-back particle correlations for top and antitop
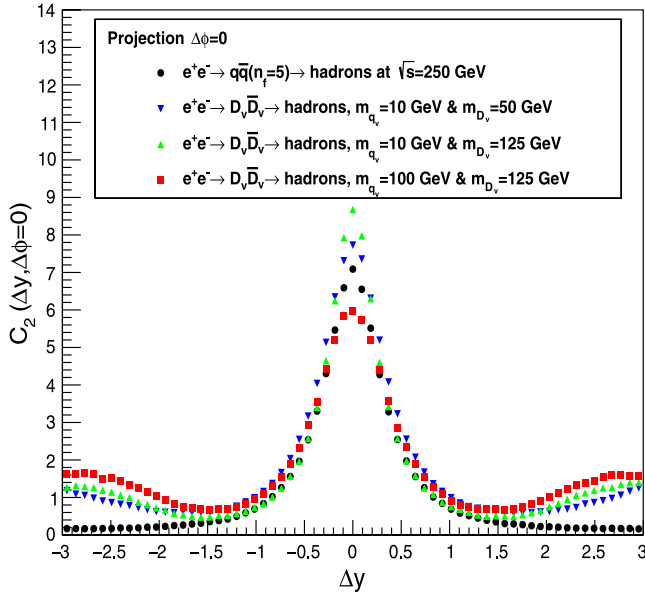
FIG. 2. $\Delta\phi \approx 0$-plane cuts of all panels of Fig. 1.

pairs because both decay promptly by electroweak interaction into lighter SM quarks that can, in its turn, hadronize. No near-side ridge should be expected, however, from the top quark jets since only SM-like parton splittings can occur. Nevertheless, back-to-back correlations are stronger in $e^+e^- \to D_v\bar{D}_v \to$ hadrons (right panel) because the HV mediator D_v can radiate QCD gluons and, in addition, decay into mass asymmetric pairs, as explained above.

For completeness, Fig. 4 shows the $\Delta\phi \approx 0$-plane cuts of both panels in Fig. 3, and, on top, the standard model $e^+e^- \to q\bar{q} \to$ hadrons and HV $e^+e^- \to q_v\bar{q}_v \to$ hadrons via Z_v-exchange. There again, the ridge takes its highest value for D_v pair production as compared to other cases. Conversely, the Z_v-exchange channel shows similar trends

compared to the SM lightest quarks since it decays into mass symmetric v-quark pairs. Finally, the top quark somewhat mimics a critical stage of matter towards the existence of such a ridge.

## B. Three-particle azimuthal correlations

As is known [25], three-particle (and higher-order) correlations provide extra information on the formation and evolution of matter in high-energy collisions. In what follows, the function of four variables:

$$
\begin{aligned}
C_3(\Delta y_{12}, &\Delta y_{13}; \Delta\phi_{12}, \Delta\phi_{13}) \\
&= \frac{S_3(\Delta y_{12}, \Delta y_{13}; \Delta\phi_{12}, \Delta\phi_{13})}{B_3(\Delta y_{12}, \Delta y_{13}; \Delta\phi_{12}, \Delta\phi_{13})}
\end{aligned} \tag{2}
$$

is used to study three-particle correlations. Again, the numerator represents the signal as it takes into account the number of particle triplets from the same event, while the denominator corresponds to the background, i.e., particle triplets from different events.

The present study is restricted to azimuthal correlations following the findings of [3] where it was concluded that azimuthal distributions are more sensitive to the presence of hidden sectors than (pseudo)rapidity distributions. Therefore, and for the sake of simplicity, the rapidity difference is fixed here to the interval $\Delta y_{12} = \Delta y_{13} = 0$, that is, particles moving with similar longitudinal rapidity (along the sphericity axis of each event).

Figure 5 displays 3-dimensional plots obtained from Eq. (2) with $\Delta y_{12} = \Delta y_{13} = 0$ at $\sqrt{s} = 800$ GeV for the SM lightest quarks (left panel) and T_v pair-production (right panel). The central peaks exhibit the existence of highly correlated collinear particle triplets whereas "satellite" peaks show correlated back-to-back particles with respect to collinear particle pairs, as stressed below.
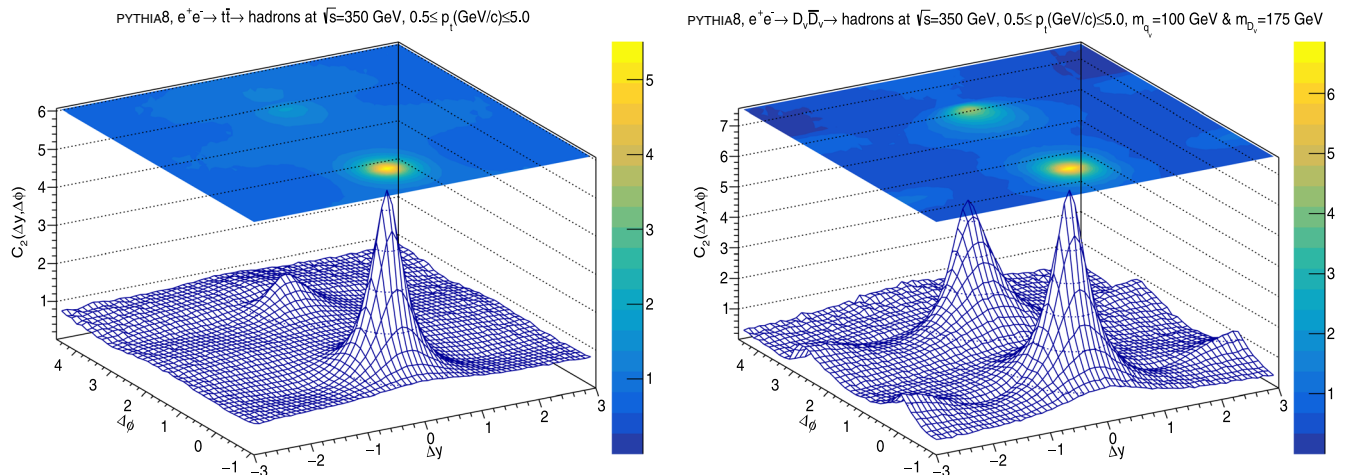
FIG. 3.   The same as in Fig. 1 but at $\sqrt{s} = 350$ GeV, obtained in the SM for $t\bar{t}$ production (left panel) and the HV scenario for the process $e^+e^- \to D_v\bar{D}_v$ with $m_{q_v} = 100$ GeV and $m_{D_v} = 175$ GeV (right panel).
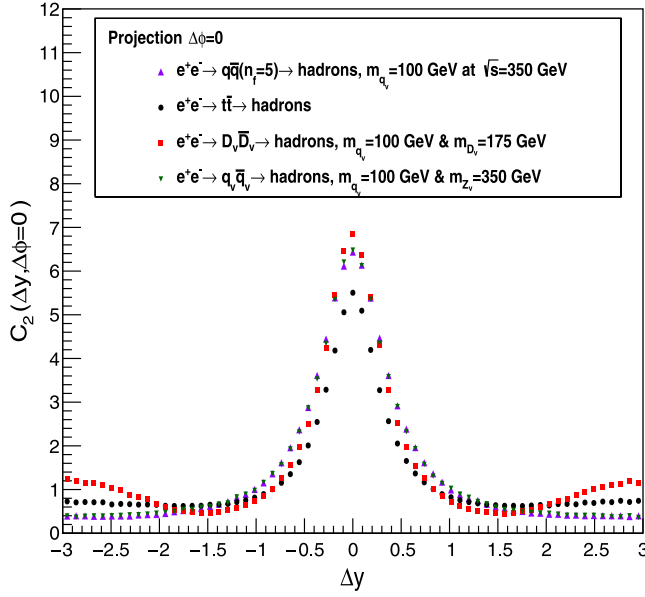
FIG. 4. $\Delta\phi \approx 0$-plane cuts of the panels of Fig. 3.

To highlight the structure obtained in Fig. 5, the contour plots of Eq. (2), i.e., $C_3(\Delta y_{12} = 0, \Delta y_{13} = 0; \Delta\phi_{12}, \Delta\phi_{13})$, are shown in Fig. 6 for light quarks (left panel), top-antitop quarks (middle panel), and $T_v\bar{T}_v$ (right panel) production with the default value $\alpha_v = 0.1$ since no significant variations were observed of both observables as the HV coupling was increased up to $\alpha_v = 0.8$. The almost independence on α_v can be understood as due to the cancellation at leading order of α_v^2 in the ratio of the correlation functions with fixed α_v-values. Indeed, the two-particle correlation function is defined as the ratio of the

double differential cross-section ($\propto \alpha_v^2$) over the product of two single differential cross-sections $\propto \alpha_v$ each one.

As mentioned above, in all three cases a rich structure can be observed on the $(\Delta\phi_{12}, \Delta\phi_{13})$-plane: the contour line *fluxes* of the central high peak together with those highlighting the *satellite* peaks linked by ridges and valleys (i.e., higher or lower values of correlations). Let us focus on the central $(\Delta\phi_{12}, \Delta\phi_{13})$-region, where the effects of the hidden sector mainly show up, while the other peaks can be interpreted as back-to back correlations of particle pairs.

Examining all three patterns shown in Fig. 6, one can immediately notice that long-range azimuthal correlations are stretched when passing from light quarks to top production and furthermore to the HV sector as areas of in-middle valleys shrink perceptively. To investigate in more detail such a behavior, one-dimensional distributions obtained from the on-diagonal ($\Delta\phi_{12} = \Delta\phi_{13}$) and off-diagonal ($\Delta\phi_{12} = -\Delta\phi_{13}$) projections of the 3-dimensional plots of Fig. 6 were plotted.

As already obtained by us in the previous studies for hadronic collisions [3,19], long-range correlations give rise to a kind of *spiderweb* structure developing in the contour plane of the three-particle correlation function. Fits were made using three Gaussian functions with widths, δ_s, δ_m, and δ_l corresponding, respectively, to: short-range correlations mainly due to resonance decays; middle-range correlations mainly due to the parton shower; and long-range correlations, attributed to the HV sector on top of the conventional cascade. From these quantities, more general widths are defined to disentangle the possible existence of a hidden sector, $\delta_M = \sqrt{\delta_s^2 + \delta_m^2}$ and $\delta_L = \sqrt{\delta_s^2 + \delta_m^2 + \delta_l^2}$, such that the former takes into account the "pure" QCD
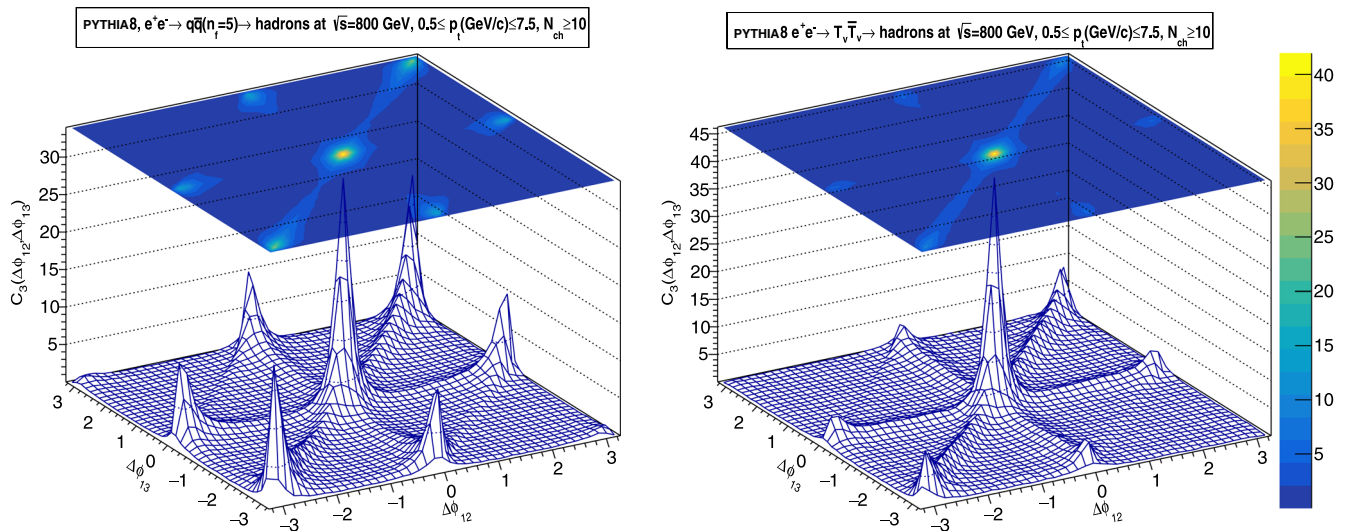

FIG. 5. Three-particle azimuthal correlations $C_3(\Delta\phi_{12}, \Delta\phi_{13})$ of charged hadrons in light quark (left panel) and $T_v\bar{T}_v$ (right panel) events in e^+e^- collisions generated with PYTHIA8 at $\sqrt{s} = 800$ GeV.
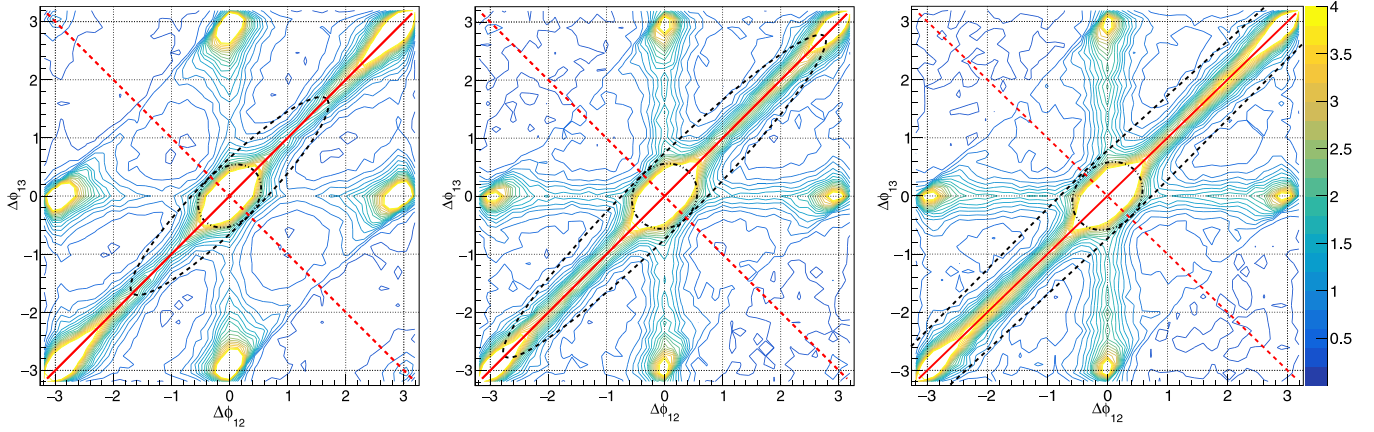
FIG. 6. Contour plot of three-particle azimuthal correlations $C_3(\Delta\phi_{12}, \Delta\phi_{13})$ of charged hadrons in light quark (left panel), top-antitop (middle panel) and $T_v\bar{T}_v$ (right panel) events in e^+e^- collisions generated with PYTHIA8 at $\sqrt{s} = 800$ GeV. The solid and dotted red lines represent the on-diagonal ($\Delta\phi_{12} = \Delta\phi_{13}$) and off-diagonal ($\Delta\phi_{12} = -\Delta\phi_{13}$) projections, respectively. Ellipses indicate long-range correlations (major axis) and middle-range correlations (minor axis), where the major axis of the inner ellipse does not include HV correlations. Long-range correlations increase from left to right while short-range and middle-range correlations remain almost unchanged as eccentricities increase. The central peak from jet correlations is cut off by the horizontal plane $C_3(\Delta\phi_{12}, \Delta\phi_{13}) = 4$, to better capture the features of the correlation function in that region.

correlations while the latter embraces all QCD and HV correlations.

III. RESULTS AND DISCUSSION

In Fig. 7, the fits for the $T_v\bar{T}_v$ case are depicted using three Gaussian functions for short-range, middle-range and long-range correlations along the on-diagonal and off-diagonal projections. Note that off-diagonal long-range correlations drop off faster than the on-diagonal ones, in

accordance with the results of [3]. The numerical values of the widths are given in Table II for all three cases, namely, $q\bar{q}$, $t\bar{t}$, and $T_v\bar{T}_v$, obtained from the Gaussian fits to the corresponding on-diagonal and off-diagonal projections of the C_3-function. Also, the mean sphericity values are given in Table II which are found to be the highest ("spherelike" events) for the HV events and the lowest ("pencil-like" events) for the lightest quarks, while the top quark events stay in between. In other words, the back-to-back hadron jets produced from the HV sector reach the most spherelike
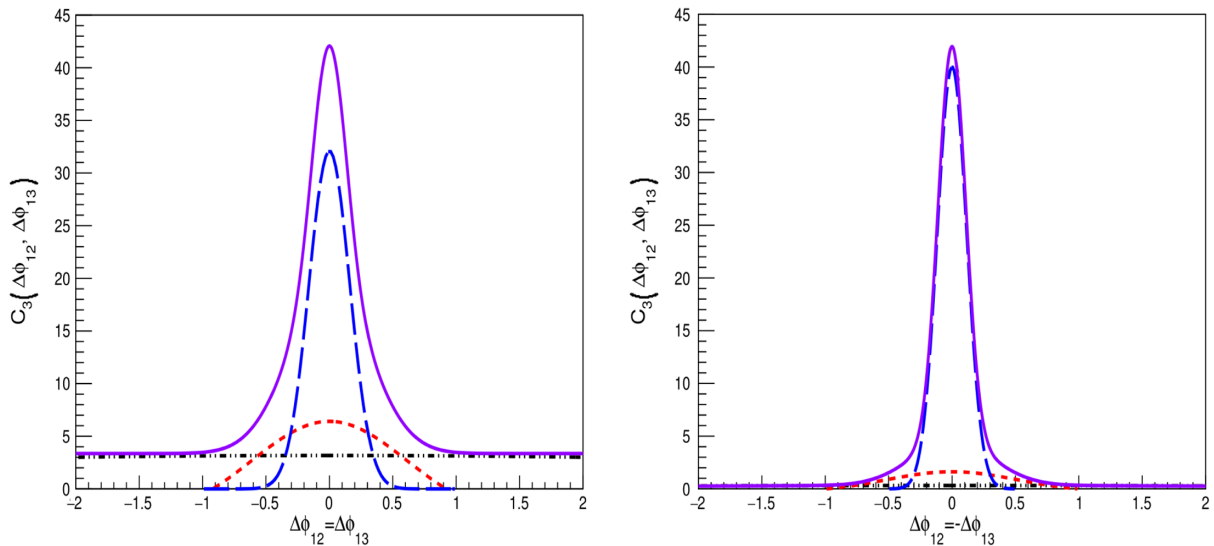

FIG. 7. On-diagonal (left panel) and off-diagonal (right panel) projections of the azimuthal contour-plot of C_3-function in the HV scenario obtained from Fig. 6 (right panel). The solid violet line represents a global fit obtained from short-range correlations (long-dashed blue line), middle-range correlations (dashed red line) and long-range correlations (dashed-dotted black line).

TABLE II.   Widths (in rad) obtained from Gaussian fits of long-range and middle-range correlations contributing to $C_3(\Delta y_{12} = 0, \Delta y_{13} = 0; \Delta\phi_{12}, \Delta\phi_{13})$ on-diagonal and off-diagonal projections (Fig. 7), along with the mean sphericity values.

v-quark species:	Light quarks	$t\bar{t}$	$T_v\bar{T}_v$
δ_L(on-diagonal)	2.36	3.89	6.16
δ_M(on-diagonal)	0.55	0.59	0.64
δ_M(off-diagonal)	0.47	0.53	0.53
Mean sphericity	0.04	0.17	0.47

shape as particles are emitted more isotropically in the event (for a recent study, see [26]).

Moreover, notice the following hierarchy involving the long-range widths shown in Table II: $\delta_L(\text{HV}) > \delta_L(t\bar{t}) > \delta_L(q\bar{q})$, highlighting the systematic enhancement of long-range correlations for nonstandard HV-initiated cascade compared to a standard one. This difference also matches the highest mean sphericity obtained for HV events. In its turn, $t\bar{t}$ production follows the same trend from $q\bar{q}$ to HV events. This is actually not a surprise because, as said above, top-quark behaves somehow like a new step from the correlation point of view.

It is also worthwhile mentioning the observed *universality* showing up for middle-range azimuthal correlations by comparing the values of δ_M for all three channels, which are quite close. This can be understood since short-range and middle-range correlations are mainly due to a conventional QCD shower, common to all channels regardless of the existence of a hidden sector on top of it.

To illustrate pictorially all the above statements, two ellipses are drawn on the contour plots of Fig. 6 for each production channel: (i) an outer ellipse whose minor/major axes numerically coincide with the $\delta_M(\text{off-diagonal})/\delta_L(\text{on-diagonal})$, and (ii) an inner ellipse with minor/major axes numerically equal to $\delta_M(\text{off-diagonal})/\delta_M(\text{on-diagonal})$, respectively, where the major axis of the inner ellipse does not include HV correlations. From inspection, similar shape (i.e., eccentricity) and size of the inner ellipses are seen for all three channels, in accordance with the above-mentioned conventional parton shower universality. On the other hand, larger eccentricities reveal the existence of a hidden sector on top of the QCD cascade. All these results are in overall agreement with our previous theoretical findings developed for hadronic collisions [3].

As a final remark, let us note that the HV signal, considered in this paper, relies on the raise of long-range azimuthal correlations, absent to the *same* extent in a conventional QCD parton shower. Nonetheless, it is known that the formation of a near-side ridge in the two-particle correlation function for hadronic collisions under certain conditions on the multiplicity and transverse momentum of the final-state particles (in the beam reference frame). Its physical origin remains still unclear although several models have been proposed to account for it. Therefore, it could be hard at first sight uncovering a new physics signal without understanding the physical origin its background in hadronic collisions. However, let us stress that the situation in e^+e^- collisions is quite different from that in hadronic collisions, since no ridge has been observed so far there [23]. Moreover, as has been seen, PYTHIA predicts much shorter angular particle correlations in pure SM processes.

IV. CONCLUSIONS

The analysis of long-range correlations in $e^+e^- \to$ hadrons collisions using PYTHIA8 event generator provides potentially observable signals on the existence of a hidden sector decaying promptly back into SM particles. On the other hand, final-state top-antitop events should provide a valuable testing ground in order to assess the net effect of a HV sector on the parton cascade. The proposed signatures, essentially consisting of longer and stronger angular correlations to be determined from the analysis of two-particle and three-particle rapidity/azimuthal correlation functions, are suggested to be seen as complementary tools in order to further contribute to the potential discovery of HV sectors at future e^+e^- colliders (and muon colliders [27]).

ACKNOWLEDGMENTS

[1] R. Perez-Ramos, V. Mathieu, and M. A. Sanchis-Lozano, Three-particle correlations in QCD parton showers, Phys. Rev. D **84**, 034015 (2011).

[2] M. A. Sanchis-Lozano, Prospects of searching for (un) particles from Hidden Sectors using rapidity correlations in multiparticle production at the LHC, Int. J. Mod. Phys. A **24**, 4529 (2009).

[3] M. A. Sanchis-Lozano and E. K. Sarkisyan-Grinbaum, Searching for new physics with three-particle correlations in pp collisions at the LHC, Phys. Lett. B **781**, 505 (2018).

[4] G. Aad *et al.*, Observation of Long-Range Elliptic Azimuthal Anisotropies in $\sqrt{s} = 13$ and 2.76 TeV pp Collisions with the ATLAS Detector, Phys. Rev. Lett. **116,** 172301 (2016).

[5] V. Khachatryan *et al.* (CMS Collaboration), Observation of long-range nearside angular correlations in proton-proton collisions at the LHC, J. High Energy Phys. 09 (2010) 091.

[6] B. Alver *et al.* (PHOBOS Collaboration), System size dependence of cluster properties from two-particle angular correlations in Cu + Cu and Au + Au collisions at $\sqrt{s_{NN}} = 200$ GeV, Phys. Rev. C **81,** 024904 (2010).

[7] E. V. Shuryak, On the origin of the 'ridge' phenomenon induced by jets in heavy ion collisions, Phys. Rev. C **76,** 047901 (2007).

[8] E. V. Shuryak, *The QCD Vacuum, Hadrons and Superdense Matter* (World Scientic, Singapore, 2004).

[9] P. Bozek and W. Broniowski, Correlations from hydrodynamic flow in p-Pb collisions, Phys. Lett. B **718,** 1557 (2013).

[10] A. Dumitru, F. Gelis, L. McLerran, and R. Venugopalan, Glasma flux tubes and the near side ridge phenomenon at RHIC, Nucl. Phys. **A810,** 91 (2008).

[11] F. Gelis, E. Iancu, J. Jalilian-Marian, and R. Venugopalan, The color glass condensate, Annu. Rev. Nucl. Part. Sci. **60,** 463 (2010).

[12] M. A. Sanchis-Lozano, E. K. Sarkisyan-Grinbaum, J. L. Domenech-Garret, and N. Sanchis-Gual, Cosmological analogies in the search for new physics in high-energy collisions, Phys. Rev. D **102,** 035013 (2020).

[13] M. J. Strassler and K. M. Zurek, Echoes of a hidden valley at hadron colliders, Phys. Lett. B **651,** 374 (2007).

[14] M. Cvetic, J. Halverson, and H. Piragua, Stringy hidden valleys, J. High Energy Phys. 02 (2013) 005.

[15] M. J. Strassler, Why unparticle models with mass gaps are examples of hidden valleys, arXiv:0801.0629.

[16] L. Carloni and T. Sjostrand, Visible effects of invisible hidden valley radiation, J. High Energy Phys. 09 (2010) 105.

[17] T. Sjöstrand, S. Ask, J. R. Christiansen, R. Corke, N. Desai, P. Ilten, S. Mrenna, S. Prestel, C. O. Rasmussen, and P. Z. Skands, An introduction to PYTHIA8.2, Comput. Phys. Commun. **191,** 159 (2015).

[18] T. Sjostrand, S. Mrenna, and P. Z. Skands, PYTHIA6.4 physics and manual, J. High Energy Phys. 05 (2006) 026.

[19] M. A. Sanchis-Lozano and E. Sarkisyan-Grinbaum, Ridge effect and three-particle correlations, Phys. Rev. D **96,** 074012 (2017).

[20] M. A. Sanchis-Lozano and E. Sarkisyan-Grinbaum, A correlated-cluster model and the ridge phenomenon in hadron–hadron collisions, Phys. Lett. B **766,** 170 (2017).

[21] G. Abbiendi *et al.* (OPAL Collaboration), Intermittency and correlations in hadronic Z^0 decays, Eur. Phys. J. C **11,** 239 (1999).

[22] C. Grupen, Multiparticle aspects of e^+e^- interactions at an energy of 133 GeV at LEP, in *Proceedings of the XXVI International Symposium on Multiparticle Dynamics (ISMD 96)* (World Scientific, Singapore, 1997) [arXiv:hep-ph/9610308].

[23] A. Badea, A. Baty, P. Chang, G. M. Innocenti, M. Maggi, C. Mcginn, M. Peters, T. A. Sheng, J. Thaler, and Y. J. Lee, Measurements of Two-Particle Correlations in e^+e^- Collisions at 91 GeV with ALEPH Archived Data, Phys. Rev. Lett. **123,** 212002 (2019).

[24] A. Abdesselam *et al.* (Belle Collaboration), Measurement of two-particle correlations in hadronic e^+e^- collisions at Belle, Report No. BELLE-CONF-2001, 2020 [arXiv:2008.04187].

[25] W. Kittel and E. A. De Wolf, *Soft Multihadron Dynamics* (World Scientific, Singapore, 2005).

[26] M. Sas and J. Schoppink, Event shapes and jets in e^+e^- and pp collisions, Nucl. Phys. **A1011,** 122195 (2021).

[27] K. R. Long, D. Lucchesi, M. A. Palmer, N. Pastrone, D. Schulte, and V. Shiltsev, Muon colliders to expand frontiers of particle physics, Nat. Phys. **17,** 289 (2021).